

# Alkali and alkali–lead oxynitride phosphate glasses: a comparative structural study by NMR and XPS

Francisco Muñoz<sup>a</sup>, Luis Pascual<sup>a</sup>, Alicia Durán<sup>a</sup>, Jean Rocherullé<sup>b</sup>, Roger Marchand<sup>b\*</sup>

<sup>a</sup> *Instituto de Cerámica y Vidrio (CSIC), Arganda del Rey, Madrid, Spain*

<sup>b</sup> *Laboratoire des verres et céramiques, UMR CNRS 6512, institut de chimie, université Rennes-1, 35042 Rennes cedex, France*

Received 15 April 2002; accepted 17 May 2002

**Abstract** – Nitrided phosphate glasses are characterized by tetrahedral units  $P(O,N)_4$  in which nitrogen atoms have substituted for both bridging and non-bridging double bonded oxygen atoms.  $^{31}P$  magic angle spinning (MAS) nuclear magnetic resonance (NMR) shows that  $PO_4$ ,  $PO_3N$  and  $PO_2N_2$  tetrahedra may coexist within the glass network. The relative proportion of these structural units as a function of the N/P ratio depends on the composition of the oxide base glass, as illustrated in sodium, lithium–sodium and lithium–sodium–lead phosphate glasses. Furthermore,  $^{31}P$  double quantum (DQ) MAS NMR shows that the nitrogen/oxygen substitution is not a random process. The modifier cations influence the connections between tetrahedra throughout the overall nitrided glass network, and, therefore, the final structure.  $N_{1s}$  X-ray photoelectron spectroscopy (XPS) shows that nitrogen atoms may exist in the  $P(O,N)_4$  tetrahedra as doubly coordinated ( $-N=$ ) and triply coordinated ( $-N<$ ) species, bonded to two and three phosphorus atoms, respectively. The relation between both kinds of nitrogen as a function of the N/P ratio depends also on the oxide-base glass composition. In this work, the thermal nitridation in flowing ammonia of alkali and alkali–lead metaphosphate glasses is studied. The results deduced from the NMR and XPS experiments make it possible, in addition to a comparison between the nitridation kinetics, to follow and to compare the structural evolution of oxynitride glasses resulting from a progressive nitrogen incorporation. In particular, the important role of PbO in the nitridation mechanism is revealed, demonstrating in this case that the nitridation is not random, its beginning included. **To cite this article:** F. Muñoz *et al.*, *C. R. Chimie 5 (2002) 731–738* © 2002 Académie des sciences / Éditions scientifiques et médicales Elsevier SAS

oxynitride glasses / nitridation / phosphates / alkali / lead /  $^{31}P$  NMR /  $N_{1s}$  XPS

**Résumé** – Les verres azotés de phosphates sont caractérisés par des entités tétraédriques  $P(O,N)_4$ , dans lesquelles les atomes d'azote ont substitué à la fois des atomes d'oxygène pontants et non pontants, doublement liés. L'étude RMN MAS du phosphore  $^{31}P$  montre que des tétraèdres  $PO_4$ ,  $PO_3N$  et  $PO_2N_2$  coexistent dans le réseau vitreux. Leur proportion relative est fonction du rapport N/P et dépend de la composition chimique du verre oxyde de base, comme il est montré dans le cas de verres de phosphates à base de sodium, lithium–sodium et lithium–sodium–plomb. Par ailleurs, l'étude RMN MAS double quanta du phosphore  $^{31}P$  montre que la substitution de l'oxygène par de l'azote ne s'effectue pas de façon aléatoire. Les cations modificateurs influencent notablement la connectivité entre les différentes unités structurales, et par là-même la structure du réseau vitreux azoté. La spectroscopie XPS  $N_{1s}$  montre que les atomes d'azote des tétraèdres  $P(O,N)_4$  peuvent être doublement ( $-N=$ ) ou triplement ( $-N<$ ) coordonnés, c'est-à-dire liés à deux ou trois atomes de phosphore. Leur proportion respective est fonction non seulement du rapport atomique N/P, mais, là aussi, de la composition du verre oxyde de base. Dans ce travail est étudiée la nituration par l'ammoniac de verres de métaphosphates alcalins et alcalins–plomb. Les résultats des études RMN et XPS permettent, en plus de la comparaison des cinétiques de nituration, de suivre et de comparer l'évolution structurale de verres oxynitrides issus de l'incorporation progressive d'azote. En particulier, le rôle du plomb dans le mécanisme de nituration est mis en évidence, démontrant ainsi que la nituration n'est pas aléatoire, y compris, dans ce cas, au début de la substitution azote/oxygène. **Pour citer cet article:** F. Muñoz *et al.*, *C. R. Chimie 5 (2002) 731–738* © 2002 Académie des sciences / Éditions scientifiques et médicales Elsevier SAS

verres azotés / nituration / phosphates / alcalins / plomb / RMN  $^{31}P$  / XPS  $N_{1s}$

\* Correspondence and reprints.

E-mail address: roger.marchand@mailhost.univ-rennes1.fr (R. Marchand).

## 1. Introduction

Phosphate glasses are of great technological interest due to specific thermal properties, i.e. low glass transition and dilatometric softening temperatures, and high thermal expansion coefficients, which make them ideal as low-temperature sealing glasses [1–5]. The problem is their low chemical durability, often associated [6]. However, the nitridation ability of these glasses under ammonia atmosphere, demonstrated as soon as 1982 [7], is a suitable way to improve their chemical resistance.

The structure of metaphosphate glasses consists of  $-\text{PO}_4-\text{PO}_4-$  chains of tetrahedra, interconnected through modifier cations. The middle tetrahedra, named  $Q^2$ -groups according to Lippma et al.'s notation [8], have two bridging oxygens (BO), bonded to neighbouring phosphorus atoms, and two non-bridging oxygens (NBO).

During nitridation in ammonia, P–N bonds form at the expense of P–O bonds, nitrogen substituting within  $\text{PO}_4$  tetrahedra for both bridging and non-bridging double-bonded oxygens to form  $\text{PO}_3\text{N}$  and  $\text{PO}_2\text{N}_2$  tetrahedra, as proved by  $^{31}\text{P}$  Nuclear Magnetic Resonance (NMR) [9, 10]. Moreover, X-ray Photoelectron Spectroscopy (XPS) results have shown that nitrogen atoms exist as two-coordinated,  $-\text{N}(\text{N}_d)$ , and three-coordinated,  $-\text{N}(\text{N}_t)$  species [10–12]. As a result of the nitrogen/oxygen substitution, the cross-linking density and the covalency of the glass network increase, which improves effectively the glass durability.

Two different models have been proposed to explain the nitridation mechanism. Reidmeyer et al. [13] have assumed that the N/O substitution is a random process. On the opposite, Le Sauze et al. [9] have described the nitridation of the  $\text{Li}_{0.5}\text{Na}_{0.5}\text{PO}_3$  glass by oxynitride microdomains growing progressively at the expense of oxide ones, where  $\text{PO}_2\text{N}_2$  tetrahedra appear by substituting preferentially bridging oxygens shared by a  $\text{PO}_4$  tetrahedron and a  $\text{PO}_3\text{N}$  tetrahedron. In both cases, it is concluded that non-bridging oxygens coordinating modifier cations are not substituted.

The higher field strength of divalent compared to monovalent modifier cations results generally in higher values of melt viscosity, which leads to a limited nitridation, for example when BaO is introduced in the starting glass formulation. PbO is an exception as its introduction provides a low melt viscosity and thus enables incorporation of high nitrogen contents, as shown by Pascual et al. [14, 15]. Moreover, the presence of  $\text{Pb}^{2+}$  cations improves the glass chemical durability while maintaining low softening points [16], thus making lead-containing glasses appropriate materials for soldering applications.

This paper deals with the thermal nitridation in flowing ammonia of alkali and alkali–lead metaphosphate glasses. In addition to a comparison between the nitridation kinetics,  $^{31}\text{P}$  Magic Angle Spinning (MAS) NMR and Double Quantum (DQ)-MAS NMR, and XPS results have been used to compare the structural evolution resulting from progressive nitrogen incorporation.

## 2. Experimental

The oxide-base glass compositions  $50 \text{ Na}_2\text{O} \cdot 50 \text{ P}_2\text{O}_5$  ('NaPO'),  $25 \text{ Li}_2\text{O} \cdot 25 \text{ Na}_2\text{O} \cdot 50 \text{ P}_2\text{O}_5$  (LiNaPO) and  $12.5 \text{ Li}_2\text{O} \cdot 12.5 \text{ Na}_2\text{O} \cdot 25 \text{ PbO} \cdot 50 \text{ P}_2\text{O}_5$  ('LiNaPbPO'), in mol%, were prepared by melting, according to a previously described procedure [17, 18]. Phosphorus oxynitride glass samples, 'NaPON', 'LiNaPON' and 'LiNaPbPON', were prepared by thermal treatment of the base glasses in flowing anhydrous ammonia, at temperatures ranging from 600 to 750 °C for times up to 96 h, as previously described [17, 18].

Nitrogen analyses were carried out in a nitrogen/oxygen LECO TC-436 analyser by the inert gas fusion method, with a maximum deviation in the N/P atomic ratio of  $\pm 0.02$ . The nitrogen content was confirmed by direct chemical analysis as  $\text{NH}_3$ , according to the Grekov method [19].

$^{31}\text{P}$  MAS NMR spectra were recorded on a Bruker ASX 100 spectrometer operating at 40.48 MHz (2.34 T). The pulse length was  $3.0 \mu\text{s}$  ( $\pi/2$ ) and 120 s delay time was used. The spinning rate was 15 kHz. The  $^{31}\text{P}$  spectra were fitted to Gaussian functions, in accordance with the chemical shift distribution of the amorphous state. The precision of the relative component determination was  $\pm 0.5\%$ .

$^{31}\text{P}$  Double Quantum MAS NMR measurements were performed at 2.34 T, using a previously described procedure [20, 21]. A 4 mm MAS probe was used at a MAS frequency of 12.5 kHz. The BaBa (back to back) sequence was applied, using TPPI (time proportional phase increment) [20–22]. A 3- $\mu\text{s}$  pulse was used ( $\pi/2$ ), and a 5 s recycling delay. Sixty-four  $t_1$  increments of 80  $\mu\text{s}$  were used, with 32 accumulations per slice.

XPS measurements were performed on a CAMECA RIBER SIA 200 electron spectrometer for multi-technique surface analysis system. This system is equipped with a MAC 2 CAMECA RIBER double stage cylindrical mirror electron-energy analyser. The photon source was a CAMECA SCX 700 dual anode X-ray source ( $h\nu = 1486.6 \text{ eV}$ ) was used as the excitation source in all cases. A spectrometer energy calibration was made by using the  $\text{Au } 4f^{7/2}$  and  $\text{Cu } 2p^{3/2}$  photo-

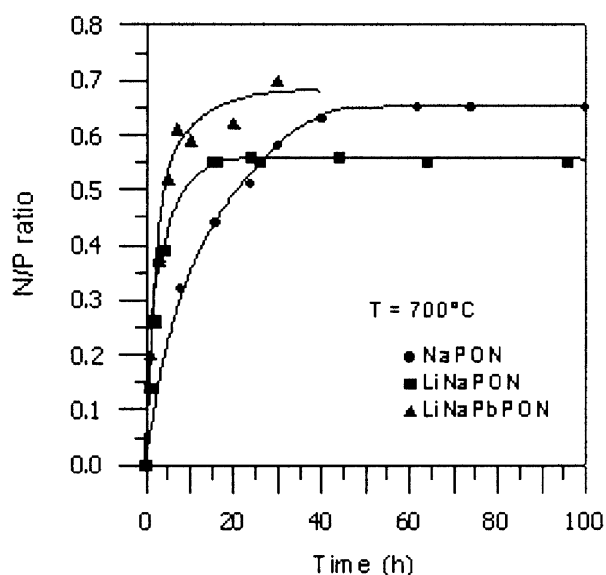


Fig. 1. Nitridation kinetics at 700 °C of NaPON, LiNaPON and LiNaPbPON glasses. The lines are only a guide for the eyes.

electron lines. Due to surface electrostatic charges detected for some samples and resulting in variable retarding effects, all the energy scales corresponding to the XPS spectra reported in this paper were normalized from the energy position of the  $C_{1s}$  photoelectron line of atmospheric carbon ( $CH_2$ ): 285 eV. The photoemission measurements were carried out on a series of samples before and after removing the surface carbon contamination by ion sputtering. The sputtering was performed for 10 min in the UHV (ultra high vacuum) analysis chamber with a 0.6 keV  $Ar^+$  ion beam ( $30 \text{ mA cm}^{-2}$ ). The elemental composition of the samples was evaluated using the integrated areas of the core-level peaks  $O_{1s}$ ,  $C_{1s}$ ,  $P_{2p}$ ,  $Pb_{4f}$ ,  $Na_{1s}$  and  $N_{1s}$ . The Li atomic concentration could not be measured due to the very low value of the ionisation cross-section for this element.

### 3. Results

#### 3.1. Nitridation kinetics

Fig. 1 shows the progressive nitrogen enrichment of NaPON, LiNaPON and LiNaPbPON glasses as a function of nitridation time at  $T = 700 \text{ °C}$ . For the three different base glasses studied, the nitrogen content reaches an asymptotic limit, which is different for each composition. The time after which this limit is reached, i.e. the nitridation rate, depends also on the starting glass composition.

#### 3.2. $^{31}P$ MAS NMR

The  $^{31}P$  MAS NMR spectra of the  $NaPO_3$ ,  $Li_{0.5}Na_{0.5}PO_3$  and  $Li_{0.25}Na_{0.25}Pb_{0.25}PO_3$  base glasses

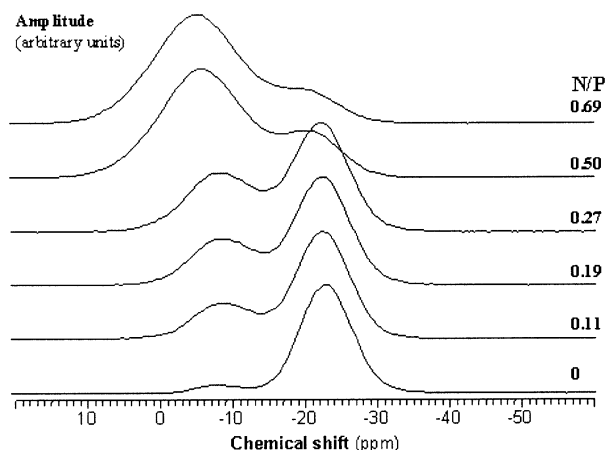


Fig. 2.  $^{31}P$  MAS NMR spectra of  $Li_{0.25}Na_{0.25}Pb_{0.25}PO_{3-3x/2}N_x$  glasses ( $0 \leq x \leq 0.69$ ).

contain a single peak at  $-20.7$ ,  $-21.4$  and  $-23$  ppm, respectively. According to Sato et al. [23], this resonance corresponds to  $Q^2$ -type sites. From the previously reported chemical shifts,  $Q^2(Na)$ :  $-19$  ppm [23],  $Q^2(Li)$ :  $-23$  ppm [9] and  $Q^2(Pb)$ :  $-24.5$  ppm [24], and considering an average distribution of the cations around the  $Q^2$  sites, we calculate  $Q^2(Li, Na)$  and  $Q^2(Li, Na, Pb)$  values of  $-21$  ppm and  $-22.8$  ppm for the  $Li_{0.5}Na_{0.5}PO_3$  and  $Li_{0.25}Na_{0.25}Pb_{0.25}PO_3$  glass compositions, respectively, in agreement with the experimental results.

As N/P increases, two new resonances can be observed in the  $^{31}P$  MAS NMR spectra of the nitrided glasses in addition to the  $Q^2$ -type resonance mentioned above, which are assigned to  $PO_3N$  ( $\sim -10$  ppm) and  $PO_2N_2$  ( $\sim 0$  ppm) tetrahedra [9, 10, 24]. As an example, Fig. 2 shows the  $^{31}P$  NMR spectra of LiNaPbPON glasses.

For the three studied series,  $PO_3N$  and  $PO_2N_2$  tetrahedra appear at the expense of  $PO_4$  tetrahedra. Fig. 3 shows the variation of the relative proportions of the three kinds of tetrahedra as a function of the N/P ratio.

The  $PO_4$  percentage (Fig. 3a) does not decrease at the same rate as the N/P ratio increases. For  $N/P < \sim 0.2$ , the proportion of remaining  $PO_4$  tetrahedra is similar for the three glass series. At higher N/P, it follows the sequence  $NaPON > LiNaPbPON > LiNaPON$ .

As shown in Fig. 3b,  $PO_3N$  tetrahedra appear as soon as nitrogen is incorporated within the glass network, and, in all cases, their proportion versus N/P increases asymptotically up to a maximum value, which depends on the starting glass composition. In the alkali phosphate glasses, the percentages of  $PO_3N$  are similar for  $N/P < \sim 0.3$ , then diverge at higher nitrogen contents to reach a maximum around 36%

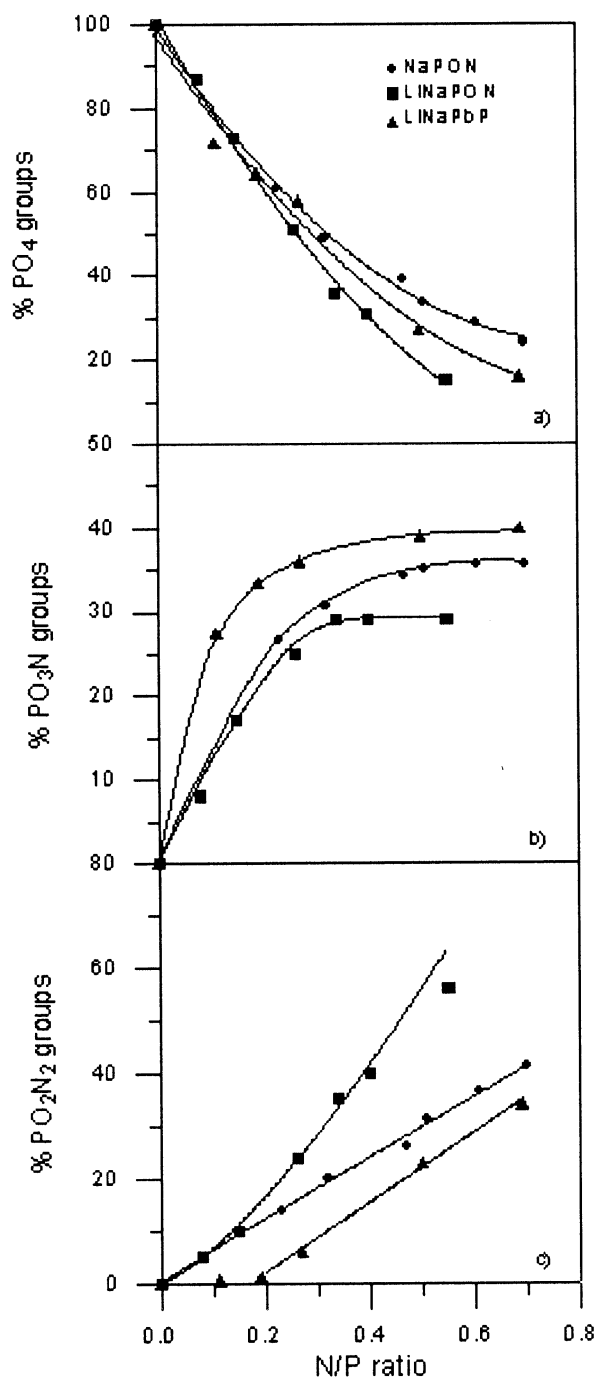


Fig. 3. Variation of the percentages of  $P(O,N)_4$  units as a function of the N/P ratio in NaPON, LiNaPON and LiNaPbPON glasses: (a)  $PO_4$ , (b)  $PO_3N$  and (c)  $PO_2N_2$  tetrahedra. The lines are only a guide for the eyes.

and 29% in NaPON and LiNaPON glasses, respectively. In LiNaPbPON glasses, much higher percentages of  $PO_3N$  are observed from the beginning of nitridation, with a final value of ~40%.

The three glass series show also a different evolution of their  $PO_2N_2$  tetrahedra when the nitrogen con-

tent increases (Fig. 3c). In NaPON and LiNaPON glasses, the percentages of  $PO_2N_2$  only coincide at low nitrogen contents (N/P ~ 0.15), their increase following a straight line for NaPON with a maximum around 41% for N/P ~ 0.7, whereas much higher percentages, around 56% for N/P = 0.55, are reached in LiNaPON glasses.

On the other hand, in LiNaPbPON glasses the  $PO_2N_2$  proportion remains close to zero for N/P < ~0.2, then increases rapidly up to a maximum of ~34% for N/P = 0.69. Whatever the considered system, the slope of the corresponding variation curve is never decreasing, even at high nitrogen contents.

### 3.3. $^{31}P$ DQ-MAS NMR

The  $^{31}P$  DQ MAS-NMR spectrum of the  $Li_{0.5}Na_{0.5}PO_{2.17}N_{0.55}$  nitrided glass sample, which is the LiNaPON nitrogen-richest composition, is presented in Fig. 4a. In addition to an auto-correlation peak A-A, at approximately -40 ppm, which is characteristic of a dipolar connectivity between  $PO_4$  tetrahedra, it indicates connectivity between  $PO_3N$  and  $PO_2N_2$  tetrahedra (auto- and cross-correlations at -5, -15 and -22 ppm). It reveals also A-B and A-C cross-correlations, i.e. the existence of direct links between pure oxygenated  $PO_4$  tetrahedra and partially nitrided ones.

The  $^{31}P$  double quantum spectrum of the  $Li_{0.25}Na_{0.25}Pb_{0.25}PO_{2.25}N_{0.5}$  glass (Fig. 4b) shows several differences compared to the LiNaPON glass. It shows a contribution on the diagonal at -21 ppm in the MAS dimension, which can be assigned to  $PO_4$ - $PO_4$  auto-correlation. The two off-diagonal resonances at -22 and -8 ppm can be attributed to cross-correlation peaks due to connectivity between  $PO_4$  and  $PO_3N$  tetrahedra. Two other off-diagonal resonances are also detected at -8 and -5 ppm and attributed to  $PO_3N$ - $PO_2N_2$  cross-correlations. At high nitrogen content, N/P = 0.69, the  $^{31}P$  DQ-MAS NMR spectrum (Fig. 5) shows that some  $PO_4$ - $PO_4$  connections still remain along with off-diagonal peaks at -7.5 and -3 ppm, corresponding to  $PO_3N$ - $PO_2N_2$  connections. No auto-correlations  $PO_3N$ - $PO_3N$  or  $PO_2N_2$ - $PO_2N_2$  are observed in the LiNaPbPON glasses, even at the highest N/P ratios. In addition, a weak resonance is also detected on the isotropic projection, with a chemical shift of +4 ppm in the MAS dimension, which is attributed to the presence of  $Q^1$  sites of pyrophosphate-type [25].

### 3.4. $N_{1s}$ XPS

Fig. 6a,b shows the  $N_{1s}$  XPS spectra of two representative oxynitride glass compositions,  $Li_{0.25}Na_{0.25}Pb_{0.25}PO_{1.97}N_{0.69}$  (Fig. 6a) and

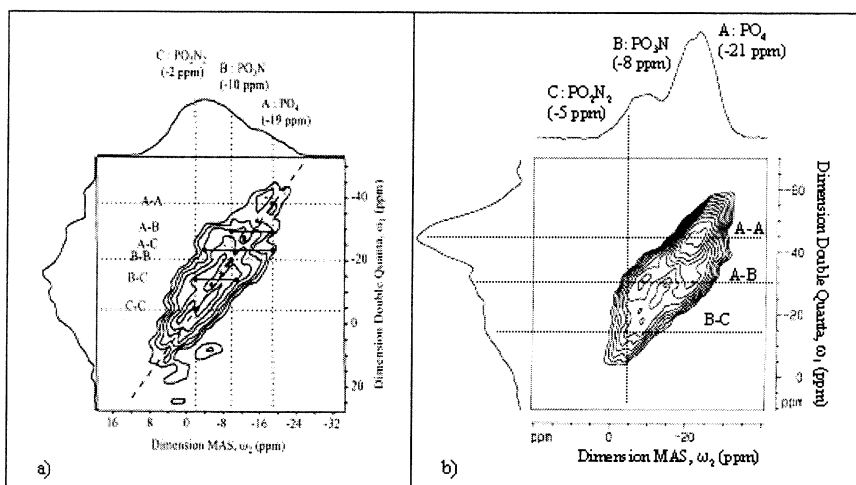


Fig. 4.  $^{31}\text{P}$  DQ-MAS NMR spectra of (a)  $\text{Li}_{0.5}\text{Na}_{0.5}\text{PO}_{2.17}\text{N}_{0.55}$  and (b)  $\text{Li}_{0.25}\text{Na}_{0.25}\text{Pb}_{0.25}\text{PO}_{2.25}\text{N}_{0.50}$  glasses.

$\text{Li}_{0.5}\text{Na}_{0.5}\text{PO}_{2.17}\text{N}_{0.55}$  (Fig. 6b), which can be decomposed into two Gaussians located at  $\sim 397.7$  and  $\sim 399.4$  eV. They have been previously assigned to the two different bonding states of nitrogen, i.e., respectively,  $-\text{N}=(\text{N}_d)$  nitrogen atoms, bonded to two phosphorus atoms, and  $-\text{N}<(\text{N}_t)$  nitrogen atoms, bonded to three phosphorus atoms [11, 12, 26, 27].

The variation of the  $\text{N}_d/\text{P}$  and  $\text{N}_t/\text{P}$  atomic ratios versus increasing N/P (as obtained by XPS) is shown in Fig. 7a and 7b for the three glass series. Both types

of nitrogen are always present from the beginning of nitridation, and in all cases the variation of  $\text{N}_d/\text{P}$  or  $\text{N}_t/\text{P}$  follows the same trend: the  $\text{N}_t$  atoms are first predominant before to become in a minority, because the slope of their variation curve decreases progressively with increasing N/P, whereas that of  $\text{N}_d$  regularly increases.

As can be seen in Fig. 8, the variation of the  $\text{N}_t/\text{N}_d$  ratio depends on the nature of the glass. Whereas a practically linear decrease is observed for the NaPON

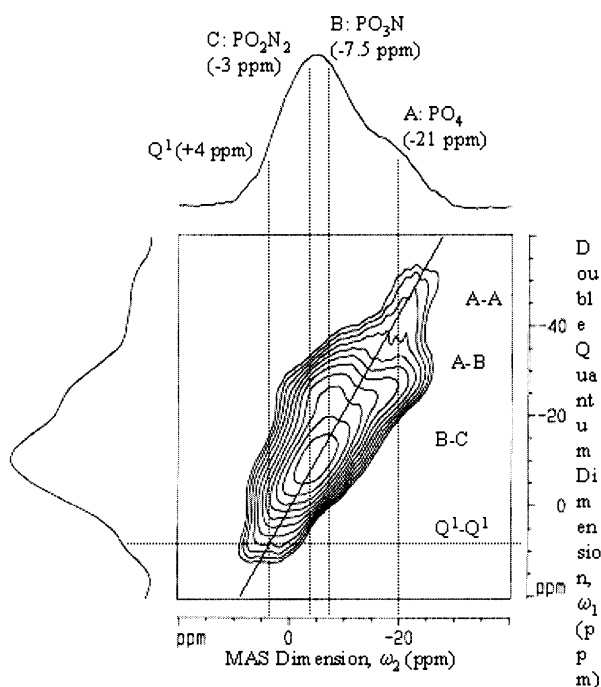


Fig. 5.  $^{31}\text{P}$  DQ-MAS NMR spectrum of the  $\text{Li}_{0.25}\text{Na}_{0.25}\text{Pb}_{0.25}\text{PO}_{1.97}\text{N}_{0.69}$  glass.

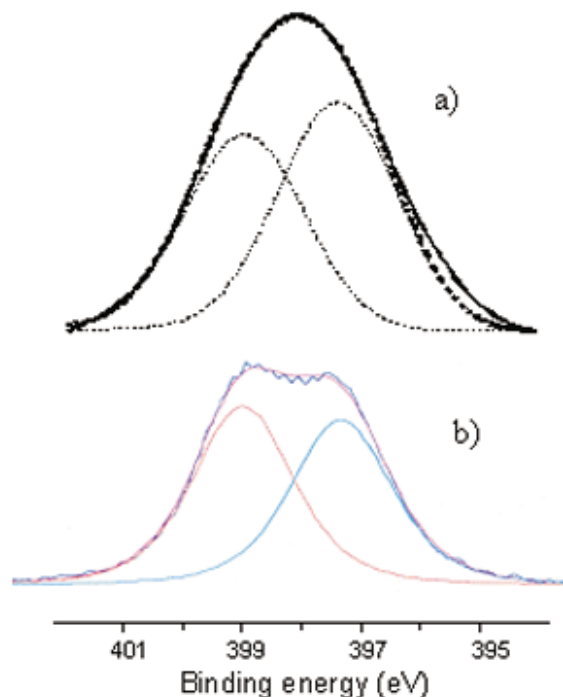


Fig. 6.  $\text{N}_{1s}$  XPS spectra of (a)  $\text{Li}_{0.25}\text{Na}_{0.25}\text{Pb}_{0.25}\text{PO}_{1.97}\text{N}_{0.69}$  and (b)  $\text{Li}_{0.5}\text{Na}_{0.5}\text{PO}_{2.17}\text{N}_{0.55}$  glass compositions.

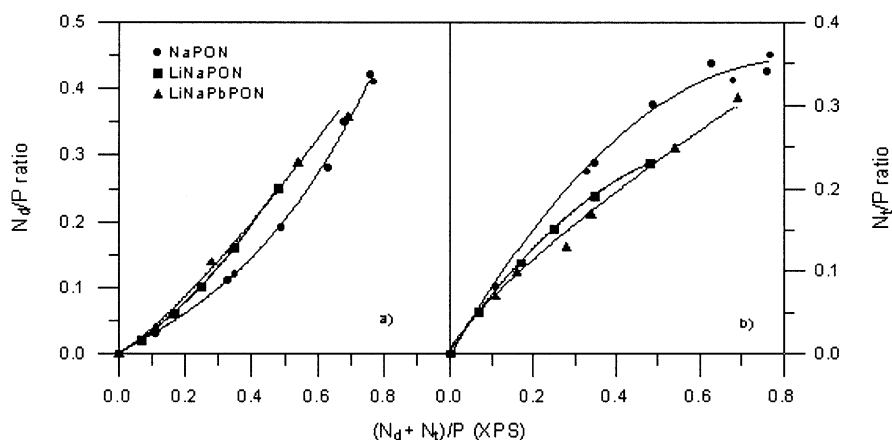


Fig. 7. (a)  $N_d/P$  ratios and (b)  $N_t/P$  ratios, versus total nitrogen content, taken from XPS data, for the three NaPON, LiNaPON and LiNaPbPON glass systems. The lines are only a guide for the eyes.

glasses, the mixed-alkali glasses, LiNaPON and LiNaPbPON give a similar variation, with in both cases a fast decrease during the first nitridation stage.

#### 4. Discussion

Fig. 1, which represents the nitridation kinetics, clearly shows a dependence on the base glass composition. On the one hand, the time after which the maximum nitrogen content is reached is shorter for LiNaPON and LiNaPbPON glasses, which have lower glass transition temperatures, and therefore lower melt viscosities, than NaPON glasses [18, 23], which is in accordance with a diffusion-controlled nitridation mechanism. On the other hand, the value of the maximum is clearly a function of the glass composition. In

particular, although the nitridation rate is higher in the less viscous LiNaPON glasses than in NaPON glasses, their maximum nitrogen content is lower.

For the three systems, the proportion of  $PO_3N$  tetrahedra as a function of the nitrogen content (Fig. 3b) reaches an asymptotic maximum value and, since that of  $PO_4$  tetrahedra decreases regularly along the whole oxynitride domain (Fig. 3a), it looks like that, from a certain N/P value,  $PO_2N_2$  tetrahedra form directly at the expense of  $PO_4$ . The interconnections between the different  $P(O,N)_4$  tetrahedra, observed by DQ-MAS NMR, imply existence of both pure oxide and oxynitride microdomains within the glass network. So, the limit in the  $PO_3N$  percentage can be explained by a nitrogen/oxygen substitution affecting preferentially bridging oxygen atoms shared by a  $PO_4$  tetrahedron and a  $PO_3N$  tetrahedron at the boundaries between microdomains. It results in a simultaneous formation of both a  $PO_3N$  and a  $PO_2N_2$  units. In other words, formation of one  $PO_2N_2$  tetrahedron at the expense of a  $PO_3N$  is accompanied by formation of another one  $PO_3N$  at the expense of a  $PO_4$ , and, consequently, the number of  $PO_3N$  tetrahedra remains constant. According to this scheme, the N/O substitution would not be a random process during the intermediate and final nitridation stages. However, a purely random substitution cannot be excluded during the first stage.

This nitridation process turns different in LiNaPbPON glasses, which is attributable, of course, to lead atoms. The fast increase in the proportion of  $PO_3N$  tetrahedra with increasing N/P, together with an absence of  $PO_2N_2$  before the maximum  $PO_3N$  percentage is reached, indicates their preferential formation at the beginning. In addition, there are neither  $PO_3N$ – $PO_3N$  nor  $PO_2N_2$ – $PO_2N_2$  connections in the corresponding DQ-MAS NMR spectra. The scheme that we propose in this case [24] assumes that, at first,  $PO_4$  tetrahedra located in the vicinity of lead atoms are preferentially nitridated and rapidly transformed into

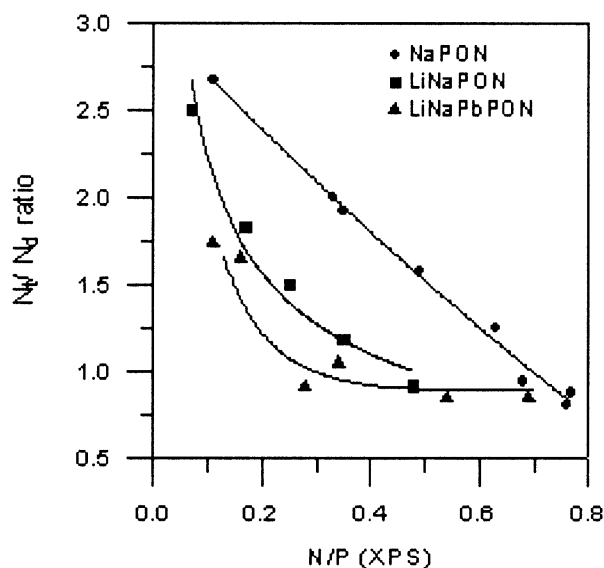


Fig. 8.  $N_t/N_d$  ratio versus total nitrogen content, taken from XPS data, for the three NaPON, LiNaPON and LiNaPbPON glass systems. The lines are only a guide for the eyes.



$\text{PO}_3\text{N}$ . Only once all of these  $\text{PO}_4$  are converted into  $\text{PO}_3\text{N}$  units, the other  $\text{PO}_4$  tetrahedra as well as the  $\text{PO}_3\text{N}$  are substituted to form  $\text{PO}_3\text{N}$  and  $\text{PO}_2\text{N}_2$  units, respectively. The high PbO concentration of the base glass along with the high coordination number of  $\text{Pb}^{2+}$  ions would explain the fast increase in  $\text{PO}_3\text{N}$  tetrahedra, as well as their higher percentage at the highest N/P ratios than in the NaPON and LiNaPON glasses.

XPS results show that the  $\text{N}_t$  species are systematically predominant at the beginning of nitridation. However, the  $\text{N}_t/\text{N}_d$  ratio decreases as a function of nitrogen content, showing a different behaviour depending on glass composition (Fig. 8). The decrease is faster for LiNaPbPON glasses. As it has been already proved [17], the  $\text{N}_t/\text{N}_d$  ratio does not depend on the melt viscosity, but it should be better correlated with structural aspects induced by the nature of modifier cations. At the beginning of nitridation, the formation of  $\text{N}_t$  nitrogen atoms, assumed to only affect bridging oxygen atoms (BO), proceeds more rapidly, probably because it is easy to replace BO atoms after the cut of P–O–P bonds within the metaphosphate chains. On the opposite, formation of  $\text{N}_d$  nitrogen atoms requires both bridging and non-bridging (NBO) oxygen atoms [12]. The progressive decrease observed in the formation rate of  $\text{N}_t$  atoms is explainable by steric effects resulting from the higher cross-linking they induce compared to  $\text{N}_d$  atoms. The faster decrease of  $\text{N}_t/\text{N}_d$  in LiNaPON and LiNaPbPON than in NaPON glasses could indicate that the greater structural complexity of a multi-cation glass network, associated to the high coordination number of large modifier cations such as  $\text{Pb}^{2+}$ , is favourable to the formation of  $\text{N}_d$  species. Further work is now in progress to clarify the structural role of lead by introducing different PbO contents in the Li–Na–Pb–P–O–N system.

On the other hand, the presence in the lead-containing glasses of  $\text{PO}_3\text{N}$  tetrahedra as the only nitrated structural units up to N/P  $\sim$  0.2 confirms that

these  $\text{PO}_3\text{N}$  tetrahedra form from the two kinds of nitrogen,  $\text{N}_d$  and  $\text{N}_t$ , since both species coexist from the very beginning of nitridation. An ideal situation for a complete understanding of the nitridation mechanism would be, of course, to closely correlate the NMR and the XPS data, for example to be able to differentiate a  $\text{PO}_3\text{N}$  tetrahedron containing a  $\text{N}_d$  atom from a  $\text{PO}_3\text{N}$  containing a  $\text{N}_t$  atom, and to distinguish also between the three different possible  $\text{PO}_2\text{N}_2$  tetrahedra.

## 5. Conclusion

In this study, a comparison was made between three different series of oxynitride phosphate glasses, NaPON, LiNaPON and LiNaPbPON, concerning their ability to nitridation and their structure, investigated by NMR and XPS. The results show that, if all the glasses are composed of  $\text{PO}_4$ ,  $\text{PO}_3\text{N}$  and  $\text{PO}_2\text{N}_2$  coexisting tetrahedral units, with both two- and three-coordinated nitrogen atoms, they can present significant differences which originate either from different melt viscosities or from structural aspects related to the nature of the modifier cations.

The nitridation mechanism proposed for LiNaPON glasses, assumed as an initial random N/O substitution followed by a progressive growing of nitrated microdomains from oxide ones, changes with introduction of lead. In this case, it is thought that the nitridation is not random since its beginning. The  $\text{Pb}^{2+}$  ions induce nitrogen/oxygen substitution in all the  $\text{PO}_4$  tetrahedra surrounding lead atoms, thus giving rise only to  $\text{PO}_3\text{N}$  tetrahedra before any formation of  $\text{PO}_2\text{N}_2$ .

The other relevant difference between these systems is the faster decrease of the  $\text{N}_d/\text{N}_t$  ratio in LiNaPON and LiNaPbPON than in NaPON glasses. This could indicate that the greater is the structural complexity of the glass network and the steric hindrance introduced by large modifier cations such as  $\text{Pb}^{2+}$ , the easier is the formation of  $\text{N}_d$  nitrogen atoms.

**Acknowledgements.** This work was financed by MCYT (Spanish Ministry of Science and Technology) through the project MAT 2000-0952-C02-01, and the Integrated Actions CSIC-CNRS 2000FR0009 and HF-2001-124. The authors wish to specially thank Drs. L. Montagne and R. Berjoan for the NMR and XPS experiments.

## References

- [1] N.H. Ray, C.J. Lewis, J.N.C. Laycock, W.D. Robinson, *Glass Technol.* 14 (2) (1973) 50.
- [2] N.H. Ray, J.N.C. Laycock, W.D. Robinson, *Glass Technol.* 14 (2) (1973) 55.
- [3] N.H. Ray, R.J. Plaisted, W.D. Robinson, *Glass Technol.* 17 (2) (1976) 66.
- [4] Y.B. Peng, D.E. Day, *Glass Technol.* 32 (5) (1991) 166.
- [5] Y.B. Peng, D.E. Day, *Glass Technol.* 32 (6) (1991) 200.
- [6] B.C. Bunker, G.W. Arnold, J.A. Wilder, *J. Non-Cryst. Solids* 64 (1984) 291.
- [7] (a) Marchand R., *C. R. Acad. Sci. Paris, Ser. II* 294 (1982) 91; (b) Marchand R., *J. Non-Cryst. Solids* 56 (1983) 173.
- [8] E. Lippma, M. Magi, A. Samoson, G. Engelhardt, *J. Am. Chem. Soc.* 102 (1980) 4889.
- [9] A. Le Sauze, L. Montagne, G. Palavit, F. Fayon, R. Marchand, *J. Non-Cryst. Solids* 139 (2000) 263–264.
- [10] B.C. Bunker, D.R. Tallant, C.A. Balfé, R.J. Kirkpatrick, G.L. Turner, M.R. Reidmeyer, *J. Am. Ceram. Soc.* 70 (9) (1987) 675.

- [11] R.K. Brow, M.R. Reidmeyer, D.E. Day, *J. Non-Cryst. Solids* 99 (1988) 178.
- [12] R. Marchand, D. Agliz, L. Boukbir, A. Quémerais, *J. Non-Cryst. Solids* 103 (1988) 35.
- [13] M.R. Reidmeyer, D.E. Day, *J. Mat. Res.* 6 (8) (1991) 1757.
- [14] L. Pascual, A. Durán, *Mater. Res. Bull.* 31 (1) (1996) 77.
- [15] L. Pascual, A. Durán, *Proc. 17th Int. Congr. Glass Beijing, China*, 5, 1995, pp. 157.
- [16] Y. He, D.E. Day, *Glass Technol.* 33 (6) (1992) 214.
- [17] A. Le Sauze, L. Montagne, G. Palavit, R. Marchand, *J. Non-Cryst. Solids* 81 (2001) 293–295.
- [18] F. Muñoz, L. Pascual, A. Durán, R. Marchand, *Phys. Chem. Glasses* (in press).
- [19] J. Guyader, F.F. Grekov, R. Marchand, J. Lang, *Rev. Chim. Min.* 15 (1978) 431.
- [20] M. Feike, R. Graf, I. Schnell, C. Jäger, H.W. Speiss, *J. Am. Chem. Soc.* 118 (1996) 9631.
- [21] K.K. Olsen, J.W. Zwanziger, P. Hartmann, C. Jäger, *J. Non-Cryst. Solids* 222 (1997) 199.
- [22] R. Ernst, G. Bodenhausen, A. Wokaun, *Principles of nuclear magnetic resonance in one and two dimensions*, Clarendon, Oxford, 1987.
- [23] R.K. Sato, R.J. Kirkpatrick, R.K. Brow, *J. Non-Cryst. Solids* 143 (1992) 257.
- [24] F. Muñoz, L. Pascual, A. Durán, L. Montagne, G. Palavit, R. Berjoan, R. Marchand, *J. Non-Cryst. Solids* (submitted).
- [25] S. Prabhakar, K.J. Rao, C.N.R. Rao, *Chem. Phys. Lett.* 139 (1) (1987) 96.
- [26] B. Wang, B.S. Kwak, B.C. Sales, J.B. Bates, *J. Non-Cryst. Solids* 183 (1995) 297.
- [27] S. Veprek, S. Iqbal, J. Brunner, M. Scharli, *Phil. Mag.* 43 (3) (1981) 527.